

## Studies on the Activity of Selected Highly Lipophilic Compounds toward hGAT1 Inhibition. Part II

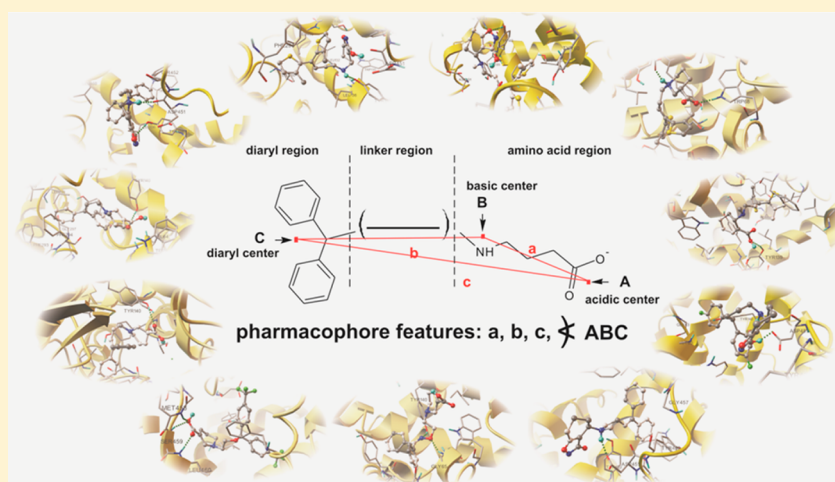
Alicja Nowaczyk,<sup>\*,†</sup> Łukasz Fijałkowski,<sup>†</sup> Magdalena Kowalska,<sup>†</sup> Adrian Podkowa,<sup>‡</sup> and Kinga Sałat<sup>§</sup>

<sup>†</sup>Department of Organic Chemistry, Faculty of Pharmacy, Collegium Medicum in Bydgoszcz, Nicolaus Copernicus University, 2 dr. A. Jurasza St., 85-094 Bydgoszcz, Poland

<sup>‡</sup>Chair of Inorganic and Analytical Chemistry, Jagiellonian University Medical College, 9 Medyczna St., 30-688 Kraków, Poland

<sup>§</sup>Department of Pharmacodynamics, Chair of Pharmacodynamics, Jagiellonian University Medical College, 9 Medyczna St., 30-688 Krakow, Poland

### S Supporting Information



**ABSTRACT:** In this paper, we describe the latest results involving molecular modeling and pharmacodynamic studies of the selected highly lipophilic compounds acting by human GABA transporter 1 (hGAT1) inhibition. The chemical interaction of 17 GABA analogues with a model of hGAT1 is described using the molecular docking method. The biological role of GAT1 is related to the regulation of GABA level in the central nervous system and GAT1 inhibition plays an important role in the control of seizure threshold. To confirm that GAT1 can be also a molecular target for drugs used to treat other neurological and psychiatric diseases (e.g., pain and anxiety), in the *in vivo* part of this study, potential antinociceptive and anxiolytic-like properties of tiagabine, a selective GAT1 inhibitor, are described.

**KEYWORDS:** Molecular docking, hGAT1, GABA, antiepileptic drugs, obsessive-compulsive disorder, neurogenic pain, mice

## INTRODUCTION

4-Aminobutanoic acid (GABA) is the main inhibitory neurotransmitter in the mammalian brain and spinal cord.<sup>1–5</sup> The GABAergic signal termination depends on its clearance by GABA transporters (GATs) which quickly remove this main inhibitory neurotransmitter from the synaptic cleft. This modulation of GABA levels highlights the importance of GATs as potential targets to regulate many physiological processes in which GABAergic transmission is involved, including seizure threshold, pain, and mood control.<sup>6–9</sup>

There is a large volume of published studies describing the GAT location in different cell types, including neurons and astrocytes, with variable expression levels across different brain regions.<sup>10</sup> Likewise, other evidence suggests that GABA could be taken up into neurons but was also actively accumulated into glial cells.<sup>11</sup> From many neuronal cell and astrocyte

culture studies, it is clear that these cells could play a significant role in the removal of GABA from the synaptic cleft. There is, however, evidence that the transport capacity for GABA cannot be characterized strictly as neuronal or glial transport GABA.<sup>11,12</sup> There is a consensus among pharmacologists for the existence of five subtypes of high-affinity GATs located on neurons and astrocytes in different species. At present, four subtypes of plasma membrane human transporters for GABA have been identified, namely: GAT1, BGT1, GAT2, and GAT3.<sup>13,14</sup> GAT1 and GAT3 have the highest expressions, being predominantly located on GABAergic nerve terminals and abundantly expressed in the mammalian central nervous

Received: June 6, 2018

Accepted: September 17, 2018

Published: September 17, 2018

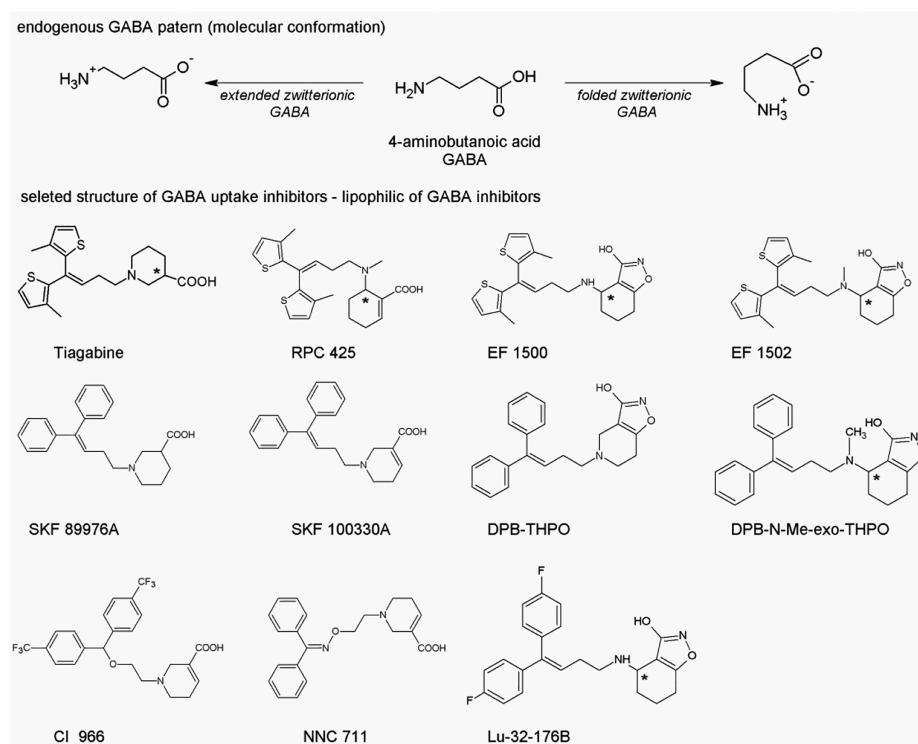


**Figure 1.** Chemical structure of the investigated compounds. Carbons at a tetrahedral stereogenic center are designated with an asterisk.

system (CNS).<sup>1,2</sup> GAT1 is a primary neuronal and some astrocyte cells GAT, while GAT3 is commonly associated with distal astrocytic site.<sup>13,15,16</sup> More recent studies have confirmed that GAT1 expression highly resembles GABAergic pathways.<sup>5,17</sup> It is noteworthy that widespread distribution of GABAergic neurons and the inhibition of GAT systems may modify seizure threshold and control the propagation of pain signals.<sup>18–20</sup>

Considering the aforementioned facts, the aim of this study is a detailed analysis of the interactions between the human GAT1 (hGAT1) and antiepileptic drugs, and active compounds and their structures. The objective of this paper is to perform the *in silico* study on the series of 17 highly lipophilic GABA uptake inhibitors. The *in silico* part describes a detailed analysis of the hydrogen bonds found in the complexes. In order to better understand the mechanism of action displayed by the tested compounds, we focused on their influence on the neurons and astrocytes cells at the molecular level. GABAergic drugs acting at various targets within the GABAergic synapses (i.e., GABAergic receptors, GAT, GABA transaminase) are widely used in medicine for the treatment of several pathologies of the central and peripheral nervous system. Apart from their wide application in epilepsy, they have been found very useful in the therapy of some nonepileptic conditions.<sup>21,22</sup> It is noteworthy that recently, a physiological level of GABA in the brain has been also found to play an important protective role in obsessive-compulsive disorder (OCD).<sup>23</sup> Although OCD is strongly related to the deficits in serotonergic neurotransmission and drugs that inhibit serotonin reuptake are considered drug treatments of choice for this disorder,<sup>24</sup> it has been also shown that reduced GABAergic activity with a concomitant excessive glutamatergic neurotransmission are present in patients suffering from OCD.<sup>23</sup>

Due to the role of GABA as the main functional component of the “pain gate” in the CNS,<sup>25,26</sup> GABAergic drugs proved their significant analgesic efficacy in many chronic pain syndromes.

Newer studies clearly indicate that GABA might be also involved in pain transduction and signal transmission in the periphery.<sup>27</sup> There is also evidence for a role of GABAergic mechanisms in the attenuation of neurogenic inflammation.<sup>28–30</sup>

In view of the above-mentioned findings, in the *in vivo* part of the present study, we aimed to assess if the inhibition of GAT1 might (1) attenuate behavioral symptoms of OCD and (2) reduce pain related to neurogenic inflammation. Since we concentrated on GAT1, for this study, as a pharmacological tool we used tiagabine, a highly selective GAT1 inhibitor. We tested it in a mouse model of OCD, namely, the marble burying test, and in a mouse model of neurogenic pain, i.e., the capsaicin test.<sup>31,32</sup> Tiagabine is an anticonvulsant drug used to treat partial seizures in humans. Recent results from clinical trials indicate that it might be also effective in patients suffering from pain<sup>33,34</sup> or mood disorders<sup>35–37</sup> but its effects on the symptoms of OCD or pain related to neurogenic inflammation have not been investigated.

## RESULTS

Figure 1 exhibits the chemical structures of studied compounds. Graphical representation of the pharmacophore model of GABA-uptake inhibitors which includes three features, i.e., A, the acidic center; B, the basic center; C, the diaryl center is shown in Figure 2. The structure of investigated compounds were compared to the proposed pharmacophore triangle by measurements of the appropriate distances and angles. All intramolecular distances and angles relevant to the pharmacophore (i.e., a, b, c,  $\angle ABC$ ), were measured and collected in Table 1. The investigated active structures of the studied compounds are compared using superimposing procedure and are shown in Figure 3. Figures 4 and 5 illustrate the binding modes between hGAT1 and 15 studied compounds. The results of docking experiments, such as the complex binding energy, specific hydrogen bond components, and hydrogen bond

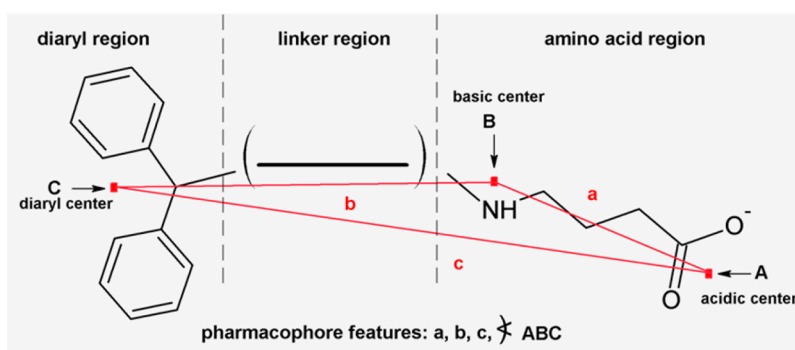


**Figure 2.** Graphical representation of the pharmacophore model of GABA-uptake inhibitors. Pharmacophore features:  $a$ ,  $b$ ,  $c$ ,  $\angle ABC$ .

**Table 1.** Distances (Å) and Angles (deg) between Pharmacophore Features for Compounds Studied in the Current Work

compd	$a$ (Å)	$b$ (Å)	$c$ (Å)	$\angle ABC$ (deg)
R-tiagabine	4.3	4.4	9.6	147
S-tiagabine	4.8	4.3	4.1	54
R-RPC 425	3.5	5.7	9.7	69
S-RPC 425	3.5	5.5	7.8	116
R-EF 1500	3.9	4.4	3.4	50
S-EF 1500	4.0	5.5	6.4	94
R-EF 1502	4.1	6.4	4.7	42
S-EF 1502	3.2	7.5	8.1	91
SKF 89976A	4.5	5.8	7.4	83
SKF 100330A	4.5	5.1	6.5	102
DPB-THPO	4.4	6.1	6.7	75
R-DPB-N-Me-exo-THPO	3.7	5.7	7.7	117
S-DPB-N-Me-exo-THPO	3.9	6.6	6.3	72
CI 966	4.3	5.4	7.6	127
NNC 711	4.1	5.1	8.8	148
R-Lu-32-176B	3.8	3.8	4.6	76
S-Lu-32-176B	3.9	4.8	3.9	56

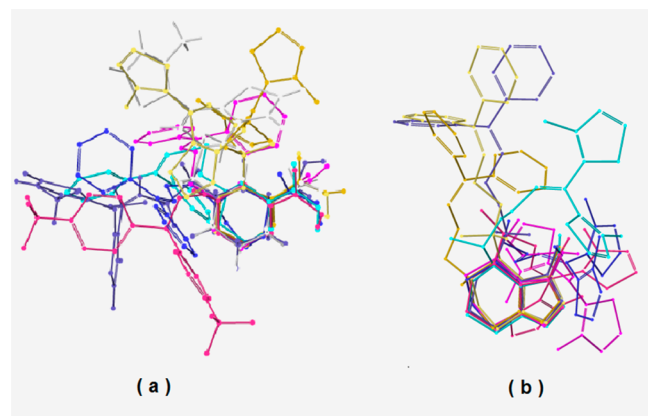


**Figure 3.** Superimposition of the investigated docked structures of (a) the nipecotic analogues and (b) the THPO analogues.

energies, lengths, and angles are shown in Supporting Information Table 1S. Figures 6 and 7 present the results of the respective pharmacological studies.

**Molecular Studies. Pharmacophore Model Analysis.** In the early 1990s, N'Goka et al. proposed the pharmacophore model for the GABA-uptake inhibitors.<sup>38</sup> According to this concept (Figure 2), it was defined as following pharmacophore regions such as amino acid, linker and diaryl regions, respectively.

The intermolecular distances and angle in the proposed pharmacophore model are as follows:  $a$ , the distance between the center of acidic and basic group;  $b$ , the distance between N nitrogen atom of amino moiety and the center of diaryl region;  $c$ , the distance between COOH group and center of diaryl ring;  $\angle ABC$ , the angle between sections  $a$  and  $b$  (specified extended-folded conformations of the studied compounds). The investigated active structures of the studied compounds are compared by means of the distances and angle listed below (Table 1). It was found that the distances between the pharmacophore features, estimated for the selected ligands, are within the following range:  $a = 3.9\text{--}5.6$  Å;  $b = 3.8\text{--}7.8$  Å;  $c = 3.4\text{--}9.7$  Å;  $\angle ABC = 42\text{--}147^\circ$ .

To obtain additional information concerning the shape of the investigated drug, the active conformations were chosen for superimposition. The atoms (except hydrogen atoms) common to these molecules were selected for the fitting procedure. Their similarity was calculated as RMS fit. The RMS routine provided estimates of how closely molecules fit to each other. The lower the RMS value, the better the similarity. The docked structures of the studied molecules were compared by superimposing them using a least-squares algorithm that minimizes the distances between the corresponding non-hydrogen atoms as shown in Figure 3. The analysis of similarity of obtained active structures shows that all 17 compounds adopt very similar conformation in the target site of the protein. The only significant deviation of the structure concerns diaryl regions.

**Molecular Docking Studies: The Glial Selective GABA Uptake Inhibitor Nipecotic Acid Group Tiagabine and RPC 425.** From the molecular docking study, it was found a little stronger interaction with hGAT1 for RPC 425 (i.e., R-RPC 425 =  $-7.95$  and S-RPC 425 =  $-7.74$  kcal/mol, respectively) than tiagabine (i.e., R-tiagabine =  $-7.23$  and S-tiagabine =  $-6.98$  kcal/mol, respectively).<sup>5</sup> The obtained results reveal that R and S enantiomers of RPC 425 form single H-bonds with hGAT1 (Figure 4). The complex of R-RPC 425-hGAT1 has one normal H-bond in which the COO<sup>-</sup> group donates energetically moderate ( $-4.13$  kcal/mol), short (2.11 Å), and nonlinear ( $164^\circ$ ) interaction to Tyr139. While the interaction between S-RPC 425 and residues of hGAT1 involve the carboxylic end of S-RPC 425 and Met458 and Ser459 that interact via bifurcated H-bond. In the bifurcated hydrogen bond the major component is Ser459 and the minor component is Met458 but in this case the associated energies are low ( $E_{\text{HB}} = -1.33$  and  $-0.60$  kcal/mol, respectively). The distances of the hydrogen bonds lie in the range from 1.84 to 2.02 Å, and due to this the three-centered hydrogen bond is not symmetric (Figure 4).



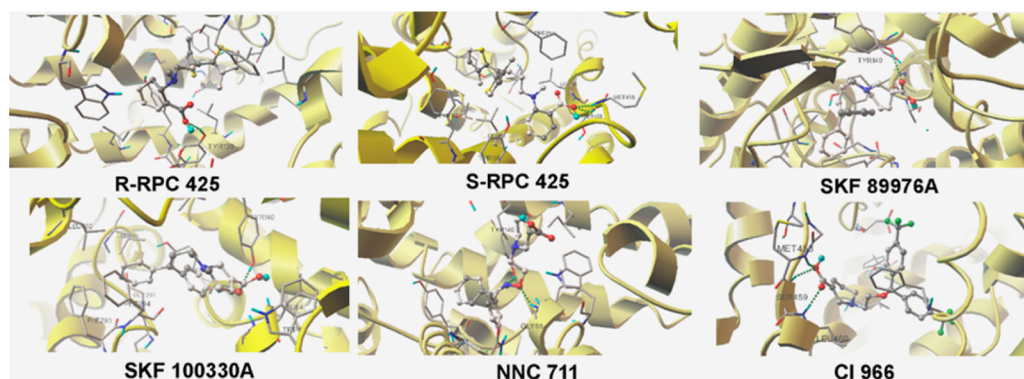


**Figure 4.** Binding modes between hGAT1 and investigated drugs RPC 425 6-(*R,S*)-((4,4-bis(3-methylthiophen-2-yl)but-3-en-1-yl)(methyl-amino)cyclohex-1-ene-1-carboxylic acid; SKF 89976A (*N*-(4,4,-diphenyl-3-butenyl)-nipecotic acid) and to guvacine yielded SKF 100330A (*N*-(4,4,-diphenyl-3-butenyl)-guvacine); NCC 711 (1-2(((diphenylmethylene)amino)oxy)ethyl)-1,2,4,6-tetrahydro-3-pyridinecarboxylic acid; CI 966 [1-[2-bis[4-(trifluoromethyl)phenyl]-methoxy]ethyl]-1, 2,5,6-tetrahydro-3-pyridine-carboxylic acid. Compound (ball and stick), residues involved in hydrogen bonding with the ligand (black) along with their hydrogen bonds (dashed green lines).

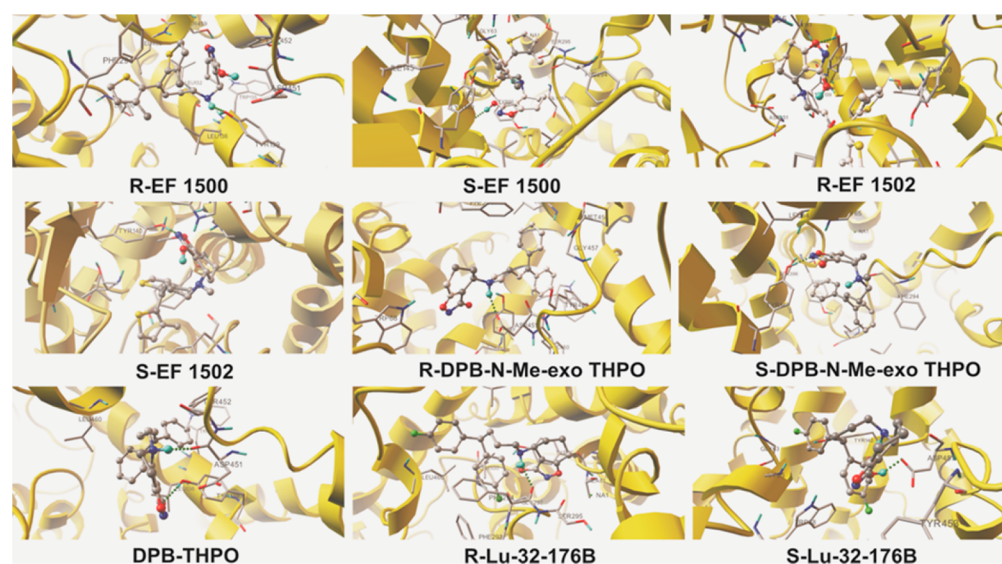


**Figure 5.** Binding modes between hGAT1 and investigated drugs: EF1500 ((*R,S*)-4-[*N*-[1,1-bis(3-methyl-2-thienyl)but-1-en-4-yl]-*N*-amino]-4,5,6,7-tetrahydrobenzo[d]isoxazol-3-ol); EF1502 ((*R,S*)-4-[*N*-[1,1-bis(3-methyl-2-thienyl)but-1-en-4-yl]-*N*-methylamino]-4,5,6,7-tetrahydrobenzo[d]isoxazol-3-ol); N-DPB-N-Me-exo-THPO: (*R,S*)-*N*-diphenylbutenyl-*N*-methyl-3-hydroxy-4-amino-4,5,6,7-tetrahydro-1,2-benzisoxazole; N-DPB-THPO: 5-(4,4-diphenylbut-3-en-1-yl)-4,5,6,7-tetrahydro[1,2]oxazolo[4,5-*c*]pyridin-3-ol; Lu-32-176B (*R,S*)-(*N*-[[4,4-diphenylbut-3-en-1-yl]amino]-4,5,6,7-tetrahydro-1,2-benzoxazol-3-ol). Compound (ball and stick) residues involved in hydrogen bonding with the ligand (black) along with their hydrogen bonds (dashed green lines).

**SKF 89976A and SKF 100330A.** It was found that both SKF 89976A (*N*-(4,4,-diphenyl-3-butenyl)-nipecotic acid) and SKF 100330A (*N*-(4,4,-diphenyl-3-butenyl)-guvacine) could interact with hGAT1 via one H-bond (Figure 4). The binding energies of SKF 89976A and SKF 100330A are  $-8.34$  and  $-7.94$  kcal/mol, respectively. As shown in Figure 4S, the carboxylic moieties of both compounds accept H-bonds. SKF 89976A creates the bifurcated bond to Met458 and Ser459, while SKF 100330A interacts via normal H-bond with Tyr140. The latest interaction involves the COO group of SKF 100330A with the oxygen atom of side-Ph-O-H of the Tyr140 residue. It is almost linear ( $177^\circ$ ) with low H-bond energies ( $-0.31$  kcal/mol). The former interaction involved in a  $\text{NH}\cdots\text{COO}\cdots\text{NH}$  bifurcated H-bond with major component of Ser459 ( $E_{\text{HB}} = -5.26$  kcal/mol,  $\theta = 160^\circ$ ) and the minor component of Met458 ( $E_{\text{HB}} = -3.46$  kcal/mol,  $\theta = 144^\circ$ ). All calculated distances of the H-bond lie in the range  $2.01$ – $2.19$  Å.

**NNC 711 and CI 966.** Both compounds can interact with hGAT1 (Figure 4). The carboxylic end of CI 966 [1-[2-bis[4-(trifluoromethyl)phenyl]-methoxy]ethyl]-1,2,5,6-tetrahydro-3-pyridinecarboxylic acid, having two oxygen atoms, forms two interactions: one oxygen is involved in a  $\text{NH}\cdots\text{O}\cdots\text{HN}$  bifurcated hydrogen bond incorporating the NH from Met458 and the NH from Ser459, while the second oxygen binds NH from Leu460 via a two-centered hydrogen bond. In the bifurcated hydrogen bond the major component is Met458 and the minor component is Ser459 but in this case the associated H-bond energies are relatively small (i.e.,  $-4.43$  and  $-3.81$  kcal/mol respectively). The distances associated with the three centered H-bonds lie in the range  $1.89$ – $2.21$  Å with  $\theta \in (149$ – $164^\circ)$  and due to this it is far from symmetric interaction. The highest hydrogen bond energy ( $-7.43$  kcal/mol) was found for the normal H-bond which is almost linear ( $171^\circ$ ). Surprisingly, the addition of (1-2(((diphenylmethylene)amino)oxy)ethyl) moiety to guvacine end-capping completely different

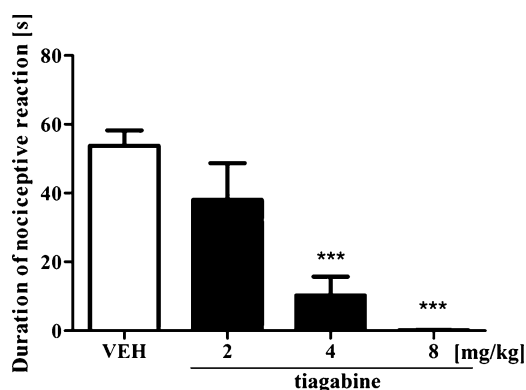


**Figure 6.** Antinociceptive effect of tiagabine in the capsaicin-induced neurogenic pain model. Results are shown as the duration of the nociceptive reaction  $\pm$  SEM. Statistical analysis: one-way analysis of variance (ANOVA), followed by Dunnett's post hoc test. Statistical significance vs vehicle-treated group: \*\*\* $p < 0.001$ . Number of animals per group:  $n = 8-10$ .

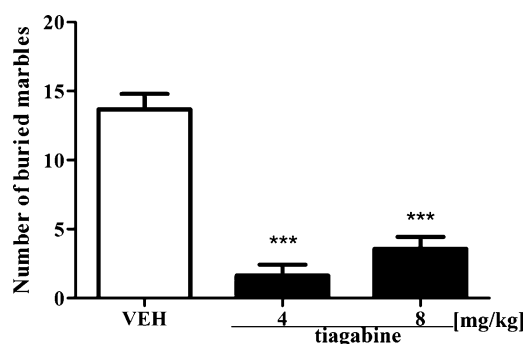


**Figure 7.** Effect of tiagabine on anxiety and obsessive-compulsive behavior measured in the marble burying test. Results are shown as the number of marbles buried  $\pm$  SEM. Statistical analysis: one-way analysis of variance (ANOVA), followed by Dunnett's post hoc test. Statistical significance vs vehicle-treated group: \*\*\* $p < 0.001$ . Number of animals per group:  $n = 8-10$ .

character of interaction with hGAT1 residue. In NNC 711-hGAT1 complex it is observed interaction between heteroatoms of the *N*-ethoxy organic function and residues of hGAT1. Both act as acceptors: the oxygen atom binds NH from Gly65 and the nitrogen atom binds OH from Tyr140. As it can be seen from Figure 4S the interactions are nonlinear ( $142^\circ$  and  $162^\circ$ ) with low H-bond energies ( $-2.44$  and  $-3.28$  kcal/mol) and comparable bond lengths ( $2.03-2.04$  Å).

**Molecular Docking Studies: The Glial Selective GABA Uptake Inhibitor THPO and Group, EF1500 and EF1502.** EF1500 ((*R,S*)-4-[*N*-[1,1-bis(3-methyl-2-thienyl)but-1-en-4-yl]-*N*-amino]-4,5,6,7-tetrahydrobenzo[d]isoxazol-3-ol). EF1502 ((*R,S*)-4-[*N*-[1,1-bis(3-methyl-2-thienyl)but-1-en-4-yl]-*N*-methylamino]-4,5,6,7-tetrahydrobenzo[d]isoxazol-3-ol).

In the preliminary analysis of the docking, it was observed that the *R* enantiomer of these compounds strongly interacts with hGAT1 (Figure 5). The interactions with the active site of the protein had binding energies of *R*-EF1500 =  $-9.19$  and *R*-EF1502 =  $9.69$  kcal/mol and *S*-EF1500 =  $-8.34$  and *S*-EF1502 =  $-8.86$ . The comparison of the obtained binding energy leads to the conclusion that all these interactions have comparable potency but slightly more potent is EF1502. The obtained results revealed that *S*-EF1502 forms two H-bonds and remainder compounds form only one. The complex of *R*-EF1500-hGAT1

has one normal H-bonding in which exocyclic amine group donates energetically moderate ( $-5.04$  kcal/mol) short ( $1.96$  Å) and nonlinear ( $150^\circ$ ) interaction to Tyr139. Similarly, the complex of *R*-EF1502-hGAT1 has one normal H-bond in which the oxygen atom of the tetrahydro-1,2-benzoxazol-3-ol ring donates energetically strong ( $-7.72$  kcal/mol), short ( $1.87$  Å), and almost linear ( $170^\circ$ ) interaction to Tyr140 (Figure 5). While the interaction between *S*-EF1500 and residues of hGAT1 involves the SER396 and exocyclic hydroxyl group donating energetically weak ( $-0.32$  kcal/mol), short ( $2.13$  Å), and almost linear ( $174^\circ$ ) interactions. The interaction of *S*-EF1502 and residues of hGAT1 involves the 4,5,6,7-tetrahydro-1,2-benzoxazol-3-ol amine group that interacts via one normal H-bond and the hydroxyl group of *S*-EF1502 that interacts via bifurcated H-bond (Figure 5). The interaction concerning the aromatic nitrogen atom of the tetrahydro-1,2-benzoxazol-3-ol ring donates one H-bond to Leu460. This interaction is almost linear (i.e.,  $167^\circ$ ) with a moderate H-bond energy ( $3.81$  kcal/mol) and a long bond length ( $2.23$  Å). Whereas the hydroxyl end of EF1502 acts as an acceptor to the NH group of MET458 and donor to the C=O of SER456's carboxyl group. From the data in Table 2S and Figure 5, it can be seen that this bifurcated system is nonlinear ( $138-148^\circ$ ), energetically and geometrically almost symmetric. The distances associated with the hydrogen bonds lie in the range from  $1.94$  to  $2.24$  Å, with a moderate energy between  $-2.62$  and  $-2.39$  kcal/mol.

**DPB-THPO and *R/S*-*N*-DPB-*N*-Me-*exo*-THPO.** DPB-THPO: 5-(4,4-diphenylbut-3-en-1-yl)-4,5,6,7-tetrahydro[1,2]oxazolo[4,5-*c*]pyridin-3-ol. *R/S*-*N*-DPB-*N*-Me-*exo*-THPO: *N*-diphenylbutenyl-*N*-methyl-3-hydroxy-4-amino-4,5,6,7-tetrahydro-1,2-benzisoxazole.

We studied *R/S*-*N*-DPB-*N*-Me-*exo*-THPO structure interaction with hGAT1 via single H-bond and DPB-THPO interaction via two normal H-bond (Figure 5). The interactions with the active site of the protein show binding energy of *R*-*N*-DPB-*N*-Me-*exo*-THPO  $\approx$  *R*-*N*-DPB-*N*-Me-*exo*-THPO  $\approx -9.5$ . In the case of the *R* enantiomer, the 4,5,6,7-tetrahydro-1,2-benzoxazol-3-ol amine group donates one normal H-bond to the C=O of the carboxyl group of ASP451. This interaction is approximately nonlinear ( $152^\circ$ ) with moderate energy, i.e.,  $-5.15$  kcal/mol and a small bond length equal  $1.91$  Å. Whereas in case of the *S* enantiomer, the oxygen atom of 4,5,6,7-tetrahydro-1,2-benzoxazol-3-ol acts as acceptor in the H-bond with TYR140. This interaction is approximately linear ( $177^\circ$ ) with low energy, i.e.,  $-2.78$  kcal/mol and a long bond length equal to  $2.23$  Å. The DPB-THPO-hGAT1 complex has a binding energy slightly less ( $-8.78$  kcal/mol) than that of *R/S*-*N*-DPB-*N*-Me-*exo*-THPO. Its H-bonds are formed between the oxygen atom of 4,5,6,7-tetrahydro-1,2-benzoxazol-3-ol ring and TYR139 and between the 4,5,6,7-tetrahydro-1,2-benzoxazol-3-ol amine group and ASP451.

***R/S*-Lu-32-176B.** *R/S*-Lu-32-176B is *R/S*-(*N*-[[4,4-diphenylbut-3-en-1-yl]amino]-4,5,6,7-tetrahydro-1,2-benzoxazol-3-ol).

The *R/S*-Lu-32-176B docking experiment revealed that this molecule can interact with the active site of the human protein models with binding energy comparable (for *R* enantiomer  $E_B = -9.09$  and for *S* enantiomer  $E_B = -9.00$  kcal/mol) to those found for *R*-EF1500 and *R*-EF1502 complex models (Figure 5). The *R/S*-Lu-32-176B-hGAT1 complex is formed via single key interaction with residues of hGAT1. In the case of the *R* enantiomer, the 4,5,6,7-tetrahydro-1,2-benzoxazol-3-ol amine group donates one normal H-bond to the C=O of the



carboxyl group of Phe295. This interaction is nearly nonlinear ( $160^\circ$ ) with low energy, i.e.,  $-2.13$  kcal/mol and a small bond length equal  $2.20$  Å. In the case of the *S* counterpart, a single interaction was found in which the 4,5,6,7-tetrahydro-1,2-benzoxazol-3-ol hydroxyl group donates to the carbonyl group of the ASP451. This interaction is approximately nonlinear ( $146^\circ$ ) with weak energy, i.e.,  $-0.61$  kcal/mol and a small bond length equal  $1.75$  Å.

**Pharmacological Part. Capsaicin Test: Neurogenic Pain Model.** Compared to vehicle, tiagabine showed antinociceptive properties in mice ( $F_{(3,37)} = 19.07$ ,  $p < 0.0001$ ). At doses of 8 and 4 mg/kg, it significantly reduced the nociceptive reaction in mice by over 99% ( $p < 0.001$ ) and 80% ( $p < 0.001$ ), respectively. At the lowest dose tested (2 mg/kg), tiagabine reduced the duration of nociceptive response in mice, but this effect was not statistically significant (Figure 6).

**Marble Burying Test: Obsessive-Compulsive Disorder Model.** In the marble burying test, tiagabine exerted a potent anxiolytic-like activity reducing obsessive-compulsive behavior of mice ( $F_{(2,27)} = 38.50$ ,  $p < 0.0001$ ). Compared to the vehicle-treated group, it significantly reduced the number of buried marbles: at the dose of 8 mg/kg by 73% ( $p < 0.001$ ) and at the dose of 4 mg/kg by 88% ( $p < 0.001$ ) (Figure 7).

## DISCUSSION

Notwithstanding that today potent and selective GAT1 inhibitors are available, it is widely accepted that structural requirements for compounds acting as inhibitor of GABA uptake are not clearly understood. The amino acid pharmacophore region is the GABA mimic part which reflect the zwitterion form of the GABA analogues (Figure 1). It was found that GABA is transported by GAT in a somewhat folded conformation with less than  $5$  Å separation of charged centers. It was recommended that approximate separation of the *a* distance can be sorted as follows: glial ( $a > 1.6$  Å), neuronal and glial ( $a < 5.0$  Å), and neuronal ( $a > 5.4$  Å) of blocking effect in selective inhibitions. By incorporation of the basic ( $-\text{NH}_2$ ) or acid ( $-\text{CO}_2\text{H}$ ) moieties of GABA into ring structures, it has been possible to immobilize different parts of the molecules and, furthermore, to develop zwitterionic GABA analogues with protolytic properties making penetration of the blood-brain barrier (BBB) possible. Previously, it was discovered that a number of cyclic amino acids, such as nipecotic acid, isonipecotic acid, guvacine, and isoguvacine, which can be considered as conformationally restricted GABA analogues, display in vitro activity as inhibitors of [ $^3\text{H}$ ]-GABA uptake.<sup>38</sup> However, a detailed investigation of these compounds revealed that these cyclic amino acids do not readily cross the BBB. Interestingly, nipecotic acid was described as potent GAT inhibitor with no affinity to the receptors. These observations have inspired researchers to search for diaryl bioisosters of GABA with higher lipophilic profiles, i.e., lipophilic binding region (preferably diheterocyclic). Together with a linker region located between the amino acid and the lipophilic region. This initiated many syntheses of structurally related lipophilic GABA compounds and led to the discovery, in 1988, of a highly lipophilic GABA uptake inhibitor with CNS activity, i.e., tiagabine ((*R*)-1-[4,4-bis(3-methyl-2-thienyl)-3-butenyl]-3-piperidine-carboxylic acid). Tiagabine is the only GABA transport inhibitor that has been approved as a drug present a therapeutic advantage in the anticonvulsant and analgesic therapies.<sup>39</sup> The result of pharmacophore analysis for all studied compounds show that the *a* distance values are in range of references for glial

transport data (Table 1). It interacts with both neuronal and glial transport sites for GABA, although much more strongly with the glial site. In addition, the received angles are far from extended conformation, and this indicates that they play a role in biological activation. The superimposition results shows that all 17 compounds adopt very similar conformation in the target site of the protein. Based on this we can treat the geometries of drugs obtained in this study as the active conformation for the investigated compounds.

Discovery of guvacine and *R*- and *S*-nipecotic acid enabled the use of them as the GABA mimetic moiety in the synthesis of more potent GAT inhibitors in which the length and electronegativity of the linker was altered along with the diaromatic region at the end of the linker. The addition of the 4,4-bis(3-methylthiophen-2-yl)but-3-en-1-yl group to nipecotic acid yielded tiagabine.<sup>5,40</sup> However, clinical use of tiagabine is limited by its short half-life and side effects (dizziness, fatigue, confusion, tremor, ataxia, and nervousness).<sup>41</sup> These observations have inspired researchers to search for new promising lead structures.<sup>42</sup> One of them is  $\beta$ -alanine, a selective but relatively weak inhibitor of glial GABA uptake.<sup>43</sup> Throughout the years, the  $\beta$ -amino acid backbone of  $\beta$ -alanine have been used for a number of lipophilic GABA analogues such as RPC 425, i.e., 6-((4,4-bis(3-methylthiophen-2-yl)but-3-en-1-yl)(methyl)amino)cyclohex-1-ene-1-carboxylic acid. Tiagabine and RPC 425 differ by exchange nipecotic acid via 6-aminocyclohex-1-ene-1-carboxylic acid and are structurally closely related to each other (Figure 1). Additionally, in tiagabine the chiral center is the carbon atom  $\alpha$  to the carboxyl group but in RPC 425 the chiral center is the carbon atom  $\alpha$  to the amino group. The detailed analysis of the docking study of tiagabine were presented in our previous work.<sup>5</sup> A number of pharmacological facts, such as a 2-fold higher selectivity for astrocytic GAT compared to neuronal<sup>44</sup> with our pharmacophore analysis (Table 1, for *R* and *S* tiagabine  $a < 5$  Å), make more understandable its higher selectivity for astrocytic GAT. In the in vivo part of the present study, using two behavioral assays, i.e., the capsaicin test and the marble burying test, we have shown that tiagabine, by inhibiting GAT1, (1) effectively attenuates pain related to neurogenic inflammation and (2) is able to reduce severity of OCD-like symptoms in mice exposed to stressful conditions (here: unfamiliar objects in the environment). Simultaneously, the results obtained indicate that GAT1 might be a potential drug target for agents that are useful in the treatment of neurogenic pain and OCD.

In contrast, RPC 425 was found to be 7-fold more selective inhibitors of the BGT1 GABA-transporter subtype than GAT1.<sup>45,46</sup> The BGT1 is expressed at much lower levels in the brain and has primarily been assigned to the astrocytes.<sup>47</sup> It is widely accepted that BGT1 plays an important role for inactivation of GABA as neurotransmitter<sup>12,48</sup> but due to very low expression levels in the brain (approximately 100–1000 times lower than GAT1) its functional role in seizure control is controversial.<sup>42</sup> Obtained pharmacophore results for the distance *a* of the RPC 425 (Table 1,  $a = 3.5$  Å) strongly support its high affinity for astrocytes. Docking data support the hypothesis that RPC 425 could interact not only with BGT1 but also with GAT1, and in a dose dependent manner due to its half maximal inhibitory concentration data (BGT1  $\text{IC}_{50} = 45$   $\mu\text{M}$ , GAT1  $\text{IC}_{50} = 307$   $\mu\text{M}$ ).<sup>45,46</sup>

The addition of 4,4-diphenyl-3-butenyl side chains to nipecotic acid yielded SKF 89976A (*N*-(4,4-diphenyl-3-butenyl)-nipecotic acid) and to guvacine yielded SKF 100330A (*N*-(4,4-diphenyl-3-butenyl)-guvacine) with the highest potency at the human

GAT1. Both compounds were potent competitive inhibitors of GABA uptake and were not substrates for the carriers.<sup>11</sup> Each agent was 20-fold more potent than the cognate parent compound in competing GABA interaction with carriers in rat diencephalic membranes. Pharmacological studies indicate that the family of compounds represented by SKF 89976A and SKF 100330A may have clinically relevant anticonvulsant activity.<sup>49</sup>

N-Alkylation of guvacine to yield [1-[2-bis[4-(trifluoromethyl)phenyl]-methoxy]ethyl]-1, 2,5,6-tetrahydro-3-pyridine-carboxylic acid, i.e., CI 966, and (1-2(((diphenylmethylene)amino)oxy)ethyl)-1,2,4,6-tetrahydro-3-pyridinecarboxylic acid, i.e., NNC 711, agents slightly more potent than guvacine at inhibiting GABA uptake. It was estimated that the NNC 711 is 50–200-fold more potent than *R,S*-nipecotic acid and guvacine. The NNC 711 was 85-fold more potent than the pattern compound guvacine in inhibiting GABA uptake into a crude synaptosome preparation and remains the most potent GABA uptake inhibitor reported to date.<sup>16,50</sup> As an inhibitor of GABA transport, it is found to have 40 000-fold higher selectivity for GAT1 compared to GAT3.<sup>16</sup> CI 966 exhibited potent anticonvulsant activity in several rodent models of seizure.<sup>11</sup> CI 966 and NNC 711, like tiagabine, have as 2-fold higher selectivity for astrocytic GAT compared to the neuronal one.<sup>1</sup> CI 966 was investigated as potent anticonvulsant, anxiolytic and neuroprotective medication but due to the serious incidence of several adverse effects at higher doses these works were stopped.<sup>40</sup> Moreover, it was found that tiagabine at the same dosage did not expose the same adverse effects.<sup>51</sup> Merging the above-mentioned docking data with pharmacological results indicates that the differences in the interactions nature of hGAT1 residues with CI 966 and NNC 711 and tiagabine failed clinical tests of CI 966. On the other hand some researchers admit possibility that the initial doses of CI 966 studied in humans were too high.<sup>51</sup>

EF1502 is a structural hybrid of tiagabine and N-Me-exo-THPO.<sup>52</sup> EF1502 was found to possess a reasonably potent and broad-spectrum anticonvulsant profile and a protective index comparable to that of the selective GAT1 inhibitor tiagabine.<sup>53</sup> The *R*-EF1502 is approximately 20-fold more potent than *S*-EF1502. But the racemic mixture EF1502 equipotently inhibits astrocytic and neuronal GAT. The EF1502 inhibits both GAT1 and BGT1<sup>53</sup> and it is subsequently reported to act synergistically with the GAT1 inhibitor tiagabine in protection against seizures. Historically, these observations were considered as evidence for functional role for BGT1 in seizure control.<sup>12,31,42</sup> These pharmacological data are in agreement with our pharmacophore analysis. As can be seen from Table 1, the distances  $a > 4 \text{ \AA}$  prove strong interaction to astrocyte cells. Combination of the above-mentioned pharmacological data with our docking data indicates that an anticonvulsant component appears with a high affinity to hGAT1.

The introduction of the lipophilic diaromatic side chain 4,4-diphenylbut-3-en-1-yl (DPB) at these compounds gave very potent GABA uptake inhibitors. The DPB substituted THPO and N-Me-exo-THPO compounds were competitive and noncompetitive inhibitors, respectively at GAT1. DPB-THPO displayed a 30-fold higher inhibitory activity than the parent compound with regard to GABA transport by GAT1 and did not display proconvulsant activity.<sup>11</sup> Additionally, it is about 4-fold more potent to astrocytic than neuronal transporter.<sup>54</sup>

Lu-32-176B, like tiagabine, is a highly selective GAT1 blocker, with 2-fold higher selectivity for astrocytic GAT compared to the neuronal one, and in combination with EF1502 it exerted a

synergistic anticonvulsant effect at all dose mixtures.<sup>1,55</sup> The last-mentioned studies, indicating another prove a functional role for BGT1 in the control of neuronal excitability and possible utility for contributed to the anticonvulsant activity of EF1502.<sup>52</sup> Additionally the Lu-32-176B as well as EF1500, both of which are lipophilic analogs of exo-THPO, did not display any affinity for mGAT2-4.

## CONCLUSION

Modern research delivers novel solutions and new potential therapeutic targets. About 30 years ago, it was assumed that astrocytes participate in the intercellular communication processes. Currently, it is widely accepted that together with neurons astrocytes play a pivotal role in regulating normal brain functions. Nowadays, due to the fact that subpopulations of astrocytes and neurons share a complementary set of channels and receptors,<sup>45</sup> the role of astrocytes was extended to the pathophysiological role in epilepsy and/or pain and other CNS-related disorders.<sup>46</sup> The domain of a single human astrocyte has been estimated to contact up to 2 million synapses. In human cortex, astrocytes are more than 2-fold larger in diameter than those in their rodent counterparts. The transport systems for GABA in neurons and glial cells have remarkably similar properties. GABA analogues in which the pharmacophore distance are separated by not less than about 5.4 Å selectively inhibit the neuronal transport of GABA.

Analgesic activity of GAT1 inhibitors has been shown previously.<sup>4,5,34,51</sup> Interestingly, none of these studies focused strictly on the role of GAT1 in pain resulting from neurogenic inflammation. In the present study, for the assessment of the role of GABAergic neurotransmission in this phenomenon, we used capsaicin, a Transient Receptor Potential Vanilloid subtype 1 (TRPV1) agonist.<sup>56</sup> This compound is widely regarded as a potent inducer of neurogenic inflammation by acting on subsets of primary sensory neurons expressing heat-sensitive TRPV1 channels to release proinflammatory neuropeptides, such as substance P or calcitonin gene-related peptide.<sup>57</sup>

Here, we demonstrated a strong, statistically significant, and dose-dependent antinociceptive activity of GAT1 inhibitor—tiagabine. Our results are in line with data obtained by other authors. These studies showed that GABA reduced capsaicin-induced pain sensation in humans,<sup>29</sup> while GABAergic agents, such as, e.g., sodium valproate or allopregnanolone, are able to abort neurogenic inflammation in migraine headache, block dural plasma protein extravasation and attenuate nociceptive signal transmission by enhancing GABAergic neurotransmission via GABA-A receptor-mediated mechanisms.<sup>58,59</sup> Similar to those findings, in our present study, tiagabine, by inhibiting GAT1 function, enhanced GABAergic neurotransmission, which resulted in analgesia and attenuation of neurogenic inflammation.

GABA deficits play a key role in the development of anxiety-related disorders, including OCD.<sup>58</sup> Although numerous randomized, placebo-controlled trials in OCD patients proved acute and long-term efficacy and safety of selective serotonin reuptake inhibitors, which makes them drugs of choice in the pharmacological management of OCD,<sup>60</sup> the decrease in GABAergic neurotransmission has been also linked with the development of OCD symptoms.<sup>61,62</sup>

In mice, the marble burying test is regarded as a “gold standard” behavioral model that mimics human OCD symptoms, in particular, compulsions.<sup>63</sup> This test utilizes a common behavior in mice, i.e., burying objects present in the

environment. The results obtained for tiagabine in the marble burying test show that the enhancement of GABAergic neurotransmission results in the anxiolytic-like action and a reduction of obsessive-compulsive behavior, which was also described elsewhere.<sup>4,34</sup>

Our present study showing anti-OCD properties of tiagabine in a mouse model is in line with a case report of an OCD patient that confirmed that the adjunction of tiagabine (15 mg/day) to a fluvoxamine (400 mg/day)-risperidone (1 mg/day) combination resulted in a significant attenuation of OCD symptoms. It was therefore concluded that the enhanced inhibitory GABAergic neurotransmission due to GAT1 inhibition reduces excitatory glutamatergic transmission in the corticostriato-thalamic system, which presumably constitutes the basis for OCD symptoms.<sup>64</sup>

Combination of the above-mentioned facts prove that a selective modification of GABA neurotransmission is a valuable approach to the search for new anticonvulsant, analgesic and anxiolytic drugs. Presented data of docking studies strongly support the hypothesis that the pharmacological action of the studied drugs are related to potency of their chemical interactions with hGAT1. Studied compounds exhibit higher binding energy to the hGAT1 simultaneously acting as selective inhibitors of astrocytic GABA uptake. According to the results of the present *in vivo* study, binding to the GABA transporter isoform 1 may be responsible for a potent pharmacological action.

## METHODS

**In Silico Studies.** The calculation procedures applied in the study are typical for processing of docking studies.

**Ligand Preparation.** The 3D structures of 16 compounds (Figure 1) were downloaded from the ZINC database.<sup>65</sup> Structures of these compounds were constructed using the GaussView 4.1.2 program. Subsequently, geometry optimization was carried out for each compound using the Gaussian version 09.<sup>66</sup> Finally, the Gasteiger charges were assigned to each compound using the Autodocktools program.<sup>67</sup>

**Human GAT-1 Transporter Preparation.** The protein sequence for the hGAT-1 protein was gained from the Swiss-Prot database<sup>68</sup> (accession number P30531). For generating the hGAT-1 structure, we took the alignment from Beuming et al.<sup>69</sup> This alignment has been refined using membrane protein-specific algorithms and by considering experimental data. Sequence identity between the template and the modeled sequence is 47% and according to our best knowledge this is the highest identity available now. Molecular docking was performed using the Autodock 4.2 suite of program.<sup>67</sup>

**Molecular Docking.** Molecular docking was performed using the Autodock 4.2 suite. Both the protein and ligands were saved in pdbqt format. A grid box with a dimension of  $60 \times 60 \times 60 \text{ \AA}^3$  and a grid spacing of  $0.375 \text{ \AA}$ , which is large enough for a free rotation of a ligand, was built centered on the center of the mass of the catalytic site of transporter according to place of GABA binding. The ligand binding site is formed by a shell of 12 surrounding important residues such as Tyr60, Ala61, Gly63, Gly65, Leu136, Tyr140, Phe294, Ser295, Tyr296, Gly297, Leu300, and Thr400.<sup>70</sup> The docking calculations were carried out using the Lamarckian genetic algorithm. The optimized docking parameters were set as follows: (i) the number of genetic algorithm run was 100; (ii) the population size was 150; (iii) the maximum number of energy evaluations was 250 000 per run; (iv) and the maximum number of generation in the genetic algorithm was 27 000. All other docking parameters were set at their default values. A cluster analysis was performed on the docked results using a RMS tolerance of  $2 \text{ \AA}$ . The best docking result in each case was considered to be the conformation with the lowest binding energy. Hydrogen bindings between docked potent agents and related macromolecule were analyzed using Autodock tools program ADT, version 1.5.4.<sup>71</sup>

**Pharmacological Studies. Animals and Housing Conditions.** Adult, 4-week old CD-1 male mice weighing 20–25 g were used in the behavioral tests. The mice were purchased from the animal breeding farm at the Faculty of Pharmacy, Jagiellonian University Medical College in Krakow. According to the European Parliament directive 2010/63/UE, the animals were kept in standard conditions ( $22 \pm 2 \text{ }^\circ\text{C}$ , relative humidity  $55 \pm 10\%$ , 15 ACPH) with access to food and water *ad libitum*. The light–dark cycle was 12:12. After the experiments, mice were euthanized by cervical dislocation. All the procedures concerning *in vivo* assays were approved by the Local Ethics Committee of the Jagiellonian University (ZI/40/2016).

**In Vivo Tests. Capsaicin Test: Neurogenic Pain Model.** Sixty minutes before the capsaicin test the mice were administered vehicle (1% Tween 80 solution, Sigma-Aldrich, Poland) or tiagabine (Tocris Bioscience, Germany) in a constant volume of 10 mL/kg. Immediately before the assay, a solution of capsaicin (1.6  $\mu\text{g}$  in 20  $\mu\text{L}$  0.9% saline) was injected intraplantarly into the right hind paw of each mouse. Then the animals were gently placed under glass beakers and observed for the next 5 min. The duration of the nociceptive reaction, i.e., licking, shaking, or biting the injected paw, was measured.<sup>72</sup>

**Marble Burying Test: OCD Model.** The test was performed according to a method described by Broekkamp et al.<sup>44</sup> with some minor modifications.<sup>45</sup> Briefly, the mice were placed individually into plastic cages identical to their home cages. The cages contained a 5 cm layer of sawdust and 20 black glass marbles (1.5 cm diameter) which were gently spaced in the cage, equidistant in a  $4 \times 5$  arrangement. After a 30 min testing period, the mice were removed from the cages and the number of marbles at least 2/3 buried were counted.

## ASSOCIATED CONTENT

### Supporting Information

The Supporting Information is available free of charge on the ACS Publications website at DOI: 10.1021/acchemneuro.8b00282.

Chemical structures of studied compounds; graphical representation of the pharmacophore model of GABA-uptake inhibitors; superimposition of the investigated docked structures of nipecotic and THPO analogues; distances ( $\text{\AA}$ ) and angles (deg) between pharmacophore features for compounds studied in the current work; binding modes between hGAT1 and 15 studied compounds; result of docking experiments, such as the complex binding energy, specific hydrogen bond components, hydrogen bond: energies, lengths, and angles (PDF)

## AUTHOR INFORMATION

### Corresponding Author

\*Tel: +(48)(52) 5853904. E-mail: alicja@cm.umk.pl.

### ORCID

Alicja Nowaczyk: 0000-0003-4945-2369

### Author Contributions

A.N. and Ł.F. conceived and directed the project. K.S., A.P., Ł.F., M.K., and A.N. designed the study. K.S., Ł.F., M.K., and A.P. collected the data and carried out the experiments. K.S., A.P., Ł.F., M.K., and A.N. analyzed the data. A.N., Ł.F., M.K., A.P., and K.S. interpreted the results and wrote the manuscript

### Funding

This study was supported by the research grant from the National Science Centre Grant No. 2014/15/B/NZ7/00930.

### Notes

The authors declare no competing financial interest.



## ■ ABBREVIATIONS LIST

#, hydrogen bond components: from the protein; %, hydrogen bond components: from the ligand; acc, hydrogen bond acceptor;  $E_{\text{FB}}$ , complex energy binding;  $E_{\text{HB}}$ , hydrogen bond energy; GABA, 4-aminobutanoic acid; GAT1, GABA transporter isoform 1;  $\theta$ , hydrogen bond angle; RPC 425, 6-(*R,S*)-((4,4-bis(3-methylthiophen-2-yl)but-3-en-1-yl)(methyl-amino)cyclo-hex-1-ene-1-carboxylic acid; SKF 89976A, (*N*-(4,4-diphenyl-3-butenyl)-nipeocotic acid); SKF 100330A, (*N*-(4,4-diphenyl-3-butenyl)-guvacine); NCC 711, (1-2-(((diphenylmethylene)amino)oxy)ethyl)-1,2,4,6-tetrahydro-3-pyridine-carboxylic acid; CI 966, [1-[2-bis[4-(trifluoromethyl)phenyl]-methoxy]ethyl]-1,2,5,6-tetrahydro-3-pyridinecarboxylic acid; EF1500, ((*R,S*)-4-[*N*-[1,1-bis(3-methyl-2-thienyl)but-1-en-4-yl]-*N*-amino]-4,5,6,7-tetrahydrobenzo[*d*]isoxazol-3-ol); EF1502, ((*R,S*)-4-[*N*-[1,1-bis(3-methyl-2-thienyl)but-1-en-4-yl]-*N*-methylamino]-4,5,6,7-tetrahydrobenzo[*d*]isoxazol-3-ol); *N*-DPB-*N*-Me-*exo*-THPO, (*R,S*)-*N*-diphenylbutenyl-*N*-methyl-3-hydroxy-4-amino-4,5,6,7-tetrahydro-1,2-benzisoxazole; *N*-DPB-THPO, 5-(4,4-diphenylbut-3-en-1-yl)-4,5,6,7-tetrahydro[1,2]oxazolo[4,5-*c*]pyridin-3-ol; Lu-32-176B, (*R,S*)-(*N*-[[4,4-diphenylbut-3-en-1-yl]amino]-4,5,6,7-tetrahydro-1,2-benzoxazol-3-ol)

## ■ REFERENCES

- (1) Madsen, K. K., White, H. S., and Schousboe, A. (2010) Neuronal and non-neuronal GABA transporters as targets for antiepileptic drugs. *Pharmacol. Ther.* 125, 394–401.
- (2) Madsen, K., White, H., Clausen, R. P., Frølund, B., Larsson, O. M., Krosgaard-Larsen, P., and Schousboe, A. (2007) Functional and pharmacological aspects of GABA transporters. In *Handbook of neurochemistry and molecular neurobiology*, pp 285–303, Springer, New York.
- (3) McCarson, K. E., and Enna, S. (2014) GABA pharmacology: the search for analgesics. *Neurochem. Res.* 39, 1948–1963.
- (4) Salat, K., Podkowa, A., Kowalczyk, P., Kulig, K., Dziubina, A., Filipek, B., and Librowski, T. (2015) Anticonvulsant active inhibitor of GABA transporter subtype 1, tiagabine, with activity in mouse models of anxiety, pain and depression. *Pharmacol. Rep.* 67, 465–472.
- (5) Fijałkowski, Ł., Salat, K., Podkowa, A., Zaręba, P., and Nowaczyk, A. (2017) Potential role of selected antiepileptics used in neuropathic pain as human GABA transporter isoform 1 (GAT1) inhibitors—Molecular docking and pharmacodynamic studies. *Eur. J. Pharm. Sci.* 96, 362–372.
- (6) Davydov, O. (2014) Antiepileptic Drugs Beyond Epilepsy (use of anticonvulsants in the treatment of pain syndromes). *Neurosci. Behav. Physiol.* 44, 772–778.
- (7) Jensen, T. S. (2002) Anticonvulsants in neuropathic pain: rationale and clinical evidence. *Eur. J. Pain* 6, 61–68.
- (8) Wiffen, P. J., Derry, S., Moore, R. A., Aldington, D., Cole, P., Rice, A. S., Lunn, M. P., Hamunen, K., and Kalso, E. A. (2013) Antiepileptic drugs for neuropathic pain and fibromyalgia an overview of Cochrane reviews. *Cochrane Database of Systematic Reviews*, 1–26.
- (9) Brøer, S., and Gether, U. (2012) The solute carrier 6 family of transporters. *Br. J. Pharmacol.* 167, 256–278.
- (10) Scimemi, A. (2014) Structure, function, and plasticity of GABA transporters. *Front. Cell. Neurosci.* 8, 1–13.
- (11) Clark, J., and Clark, W. (2001) Pharmacology of GABA transporters. In *Pharmacology of GABA and Glycine Neurotransmission* (Möhler, H., Ed.), pp 355–372, Springer-Verlag, Berlin.
- (12) Schousboe, A., Wellendorph, P., Frølund, B., Clausen, R. P., and Krosgaard-Larsen, P. (2017) Astrocytic GABA Transporters: Pharmacological Properties and Targets for Antiepileptic Drugs. In *Glial Amino Acid Transporters*, pp 283–296, Springer.
- (13) Conti, F., Minelli, A., and Melone, M. (2004) GABA transporters in the mammalian cerebral cortex: localization, development and pathological implications. *Brain Res. Rev.* 45, 196–212.
- (14) Schousboe, A., Madsen, K. K., Barker-Haliski, M. L., and White, H. S. (2014) The GABA synapse as a target for antiepileptic drugs: a historical overview focused on GABA transporters. *Neurochem. Res.* 39, 1980–1987.
- (15) McQuail, J. A., Frazier, C. J., and Bizon, J. L. (2015) Molecular aspects of age-related cognitive decline: the role of GABA signaling. *Trends Mol. Med.* 21, 450–460.
- (16) Borden, L. (1996) GABA transporter heterogeneity: pharmacology and cellular localization. *Neurochem. Int.* 29, 335–356.
- (17) Schousboe, A., Sarup, A., Larsson, O. M., and White, H. S. (2004) GABA transporters as drug targets for modulation of GABAergic activity. *Biochem. Pharmacol.* 68, 1557–1563.
- (18) Scimemi, A. (2014) Structure, function, and plasticity of GABA transporters. *Front. Cell. Neurosci.* 8, 1–14.
- (19) Kristensen, A. S., Andersen, J., Jørgensen, T. N., Sørensen, L., Eriksen, J., Loland, C. J., Strømgaard, K., and Gether, U. (2011) SLC6 neurotransmitter transporters: structure, function, and regulation. *Pharmacol. Rev.* 63, 585–640.
- (20) Wein, T., Petrera, M., Allmendinger, L., Höfner, G., Pabel, J., and Wanner, K. T. (2016) Different Binding Modes of Small and Large Binders of GAT1. *ChemMedChem* 11, 509–18.
- (21) Lader, M. (2005) Management of panic disorder. *Expert Rev. Neurother.* 5 (2), 259–66.
- (22) Quagliato, L. A., Freire, R. C., and Nardi, A. E. (2018) Risks and benefits of medications for panic disorder: a comparison of SSRIs and benzodiazepines. *Expert Opin. Drug Saf.* 17 (3), 315–324.
- (23) Russo, A. J., and Pietsch, S. C. (2013) Decreased Hepatocyte Growth Factor (HGF) and Gamma Aminobutyric Acid (GABA) in Individuals with Obsessive-Compulsive Disorder (OCD). *Biomarker Insights* 8, 107–14.
- (24) Goddard, A. W., Shekhar, A., Whiteman, A. F., and McDougle, C. J. (2008) Serotonergic mechanisms in the treatment of obsessive-compulsive disorder. *Drug Discovery Today* 13 (7–8), 325–32.
- (25) Benson, C., Mifflin, K., Kerr, B., Jesudasan, S. J., Dursun, S., and Baker, G. (2015) Biogenic Amines and the Amino Acids GABA and Glutamate: Relationships with Pain and Depression. *Mod. Trends Pharmacopsychiatry* 30, 67–79.
- (26) Mendell, L. M. (2014) Constructing and deconstructing the gate theory of pain. *Pain* 155 (2), 210–6.
- (27) Dadsetan, S., Balzano, T., Forteza, J., Agusti, A., Cabrera-Pastor, A., Taoro-Gonzalez, L., Hernandez-Rabaza, V., Gomez-Gimenez, B., Elmili, N., Llansola, M., and Felipo, V. (2016) Infiximab reduces peripheral inflammation, neuroinflammation, and extracellular GABA in the cerebellum and improves learning and motor coordination in rats with hepatic encephalopathy. *J. Neuroinflammation* 13, 230–245.
- (28) Malhotra, R. (2016) Understanding migraine: Potential role of neurogenic inflammation. *Ann. Indian Acad. Neurol.* 19 (2), 175–82.
- (29) Zhang, Y., Wang, K., Arendt-Nielsen, L., and Cairns, B. E. (2018)  $\gamma$ -Aminobutyric acid (GABA) oral rinse reduces capsaicin-induced burning mouth pain sensation: An experimental quantitative sensory testing study in healthy subjects. *Eur. J. Pain.* 22 (2), 393–401.
- (30) Malhotra, R. (2016) Understanding migraine: Potential role of neurogenic inflammation. *Ann. Indian Acad. Neurol.* 19 (2), 175–82.
- (31) Gazerani, P., Pedersen, N. S., Staahl, C., Drewes, A. M., and Arendt-Nielsen, L. (2009) Subcutaneous Botulinum toxin type A reduces capsaicin-induced trigeminal pain and vasomotor reactions in human skin. *Pain* 141 (1–2), 60–9.
- (32) Begnami, A. F., Spindola, H. M., Ruiz, A. L. T. G., de Carvalho, J. E., Groppo, F. C., and Rehder, V. L. G. (2018) Antinociceptive and anti-edema properties of the ethyl acetate fraction obtained from extracts of *Coriandrum sativum* Linn. leaves. *Biomed. Pharmacother.* 103, 1617–1622.
- (33) Smith, M. D., Woodhead, J. H., Handy, L. J., Pruess, T. H., Vanegas, F., Grussendorf, E., Grussendorf, J., White, K., Bulaj, K. K., Krumin, R. K., et al. (2017) Preclinical Comparison of Mechanistic

cally Different Antiseizure, Antinociceptive, and/or Antidepressant Drugs in a Battery of Rodent Models of Nociceptive and Neuropathic Pain. *Neurochem. Res.* 42, 1995–2010.

(34) Salat, K., Podkowa, A., Malikowska, N., Kern, F., Pabel, J., Wojcieszak, E., Kulig, K., Wanner, K. T., Strach, B., and Wyska, E. (2017) Novel, highly potent and in vivo active inhibitor of GABA transporter subtype 1 with anticonvulsant, anxiolytic, antidepressant and antinociceptive properties. *Neuropharmacology* 113, 331–342.

(35) Schwartz, T. L., and Nihalani, N. (2006) Tiagabine in anxiety disorders. *Expert Opin. Pharmacother.* 7, 1977–1987.

(36) Carpenter, L. L., Schecter, J. M., Tyrka, A. R., Mello, A. F., Mello, M. F., Haggarty, R., and Price, L. H. (2006) Open-label tiagabine monotherapy for major depressive disorder with anxiety. *J. Clin. Psychiatry* 67, 66–71.

(37) Pollack, M. H., Roy-Byrne, P. P., Van Ameringen, M., Snyder, H., Brown, C., Ondrasik, J., and Rickels, K. (2005) The selective GABA reuptake inhibitor tiagabine for the treatment of generalized anxiety disorder: results of a placebo-controlled study. *J. Clin. Psychiatry* 66, 1401–1408.

(38) N'Goka, V., Schlewer, G., Linget, J. M., Chambon, J. P., and Wermuth, C. G. (1991) GABA-uptake inhibitors: construction of a general pharmacophore model and successful prediction of a new representative. *J. Med. Chem.* 34, 2547–2557.

(39) Meldrum, B. S., and Rogawski, M. A. (2007) Molecular targets for antiepileptic drug development. *Neurotherapeutics* 4, 18–61.

(40) Chong, D. J., and Lerman, A. M. (2016) Practice update: review of anticonvulsant therapy. *Curr. Neurol. Neurosci. Rep.* 16, 39.

(41) Kubova, H. (2016) Side Effects of Antiepileptic Drugs. In *Antiepileptic Drug Discovery*, pp 329–350, Springer.

(42) Kempson, S. A., Zhou, Y., and Danbolt, N. C. (2014) The betaine/GABA transporter and betaine: roles in brain, kidney, and liver. *Front. Physiol.* 5, 159.

(43) Krogsgaard-Larsen, P. (1980) Inhibitors of the GABA uptake systems. *Mol. Cell. Biochem.* 31, 105–121.

(44) Madsen, K. K., Ebert, B., Clausen, R. P., Krogsgaard-Larsen, P., Schousboe, A., and White, H. S. (2011) Selective GABA transporter inhibitors tiagabine and EF1502 exhibit mechanistic differences in their ability to modulate the ataxia and anticonvulsant action of the extrasynaptic GABA<sub>A</sub> receptor agonist gaboxadol. *J. Pharmacol. Exp. Ther.* 338, 214–219.

(45) Vogensen, S. B., Jørgensen, L., Madsen, K. K., Jurik, A., Borkar, N., Rosatelli, E., Nielsen, B., Ecker, G. F., Schousboe, A., and Clausen, R. P. (2015) Structure activity relationship of selective GABA uptake inhibitors. *Bioorg. Med. Chem.* 23, 2480–2488.

(46) Vogensen, S. B., Jørgensen, L., Madsen, K. K., Borkar, N., Wellendorph, P., Skovgaard-Petersen, J., Schousboe, A., White, H. S., Krogsgaard-Larsen, P., and Clausen, R. P. (2013) Selective mGAT2 (BGT-1) GABA uptake inhibitors: design, synthesis, and pharmacological characterization. *J. Med. Chem.* 56, 2160–2164.

(47) Damgaard, M., Haugaard, A. S., Kicking, S., Al-Khawaja, A., Lie, M. E., Ecker, G. F., Clausen, R. P., and Frolund, B. (2017) Development of Non-GAT1-Selective Inhibitors: Challenges and Achievements. In *Glial Amino Acid Transporters*, pp 315–332, Springer.

(48) Hirase, H., and Koizumi, S. (2018) Astrocytes as therapeutic targets in brain diseases. *Neurosci. Res.* 126, 1–2.

(49) Yunger, L., Fowler, P. J., Zarevics, P., and Setler, P. (1984) Novel inhibitors of gamma-aminobutyric acid (GABA) uptake: anticonvulsant actions in rats and mice. *J. Pharmacol. Exp. Ther.* 228, 109–115.

(50) Suzdak, P. D., and Jansen, J. A. (1995) A review of the preclinical pharmacology of tiagabine: a potent and selective anticonvulsant GABA uptake inhibitor. *Epilepsia* 36, 612–626.

(51) Krogsgaard-Larsen, P., Frolund, B., and Frydenvang, K. (2000) GABA uptake inhibitors. Design, molecular pharmacology and therapeutic aspects. *Curr. Pharm. Des.* 6, 1193–1209.

(52) White, H. S., Watson, W. P., Hansen, S. L., Slough, S., Perregaard, J., Sarup, A., Bolvig, T., Petersen, G., Larsson, O. M., and Clausen, R. P. (2005) First demonstration of a functional role for

central nervous system betaine/ $\gamma$ -aminobutyric acid transporter (mGAT2) based on synergistic anticonvulsant action among inhibitors of mGAT1 and mGAT2. *J. Pharmacol. Exp. Ther.* 312, 866–874.

(53) Clausen, R. P., Frolund, B., Larsson, O. M., Schousboe, A., Krogsgaard-Larsen, P., and White, H. S. (2006) A novel selective  $\gamma$ -aminobutyric acid transport inhibitor demonstrates a functional role for GABA transporter subtype GAT2/BGT-1 in the CNS. *Neurochem. Int.* 48, 637–642.

(54) Bolvig, T., Larsson, O. M., Pickering, D. S., Nelson, N., Falch, E., Krogsgaard-Larsen, P., and Schousboe, A. (1999) Action of bicyclic isoxazole GABA analogues on GABA transporters and its relation to anticonvulsant activity. *Eur. J. Pharmacol.* 375, 367–374.

(55) Madsen, K. K., Clausen, R. P., Larsson, O. M., Krogsgaard-Larsen, P., Schousboe, A., and Steve White, H. (2009) Synaptic and extrasynaptic GABA transporters as targets for anti-epileptic drugs. *J. Neurochem.* 109, 139–144.

(56) Salat, K., Moniczewski, A., and Librowski, T. (2013) Transient receptor potential channels - emerging novel drug targets for the treatment of pain. *Curr. Med. Chem.* 20 (11), 1409–36.

(57) Malhotra, R. (2016) Understanding migraine: Potential role of neurogenic inflammation. *Ann. Indian Acad. Neurol.* 19 (2), 175–82.

(58) Linde, M., Mulleners, W. M., Chronicle, E. P., and McCrory, D. C. (2013) Valproate (valproic acid or sodium valproate or a combination of the two) for the prophylaxis of episodic migraine in adults. *Cochrane Database Syst. Rev.* 24 (6), CD010611.

(59) Guennoun, R., Labombarda, F., Gonzalez Deniselle, M. C., Liere, P., De Nicola, A. F., and Schumacher, M. (2015) Progesterone and allopregnanolone in the central nervous system: response to injury and implication for neuroprotection. *J. Steroid Biochem. Mol. Biol.* 146, 48–61.

(60) Goodman, W. K., Grice, D. E., Lapidus, K. A., and Coffey, B. J. (2014) Obsessive-compulsive disorder. *Psychiatr Clin North Am.* 37 (3), 257–67. Ninan, P. T. (2003) Obsessive-compulsive disorder: implications of the efficacy of an SSRI, paroxetine. *Psychopharmacol Bull.* 37 (Suppl 1), 89–96.

(61) Zai, G., Arnold, P., Burroughs, E., Barr, C. L., Richter, M. A., and Kennedy, J. L. (2005) Evidence for the gamma-amino-butyric acid type B receptor 1 (GABBR1) gene as a susceptibility factor in obsessive-compulsive disorder. *Am. J. Med. Genet., Part B* 134B (1), 25–9.

(62) Zhang, Z., Fan, Q., Bai, Y., Wang, Z., Zhang, H., and Xiao, Z. (2016) Brain Gamma-Aminobutyric Acid (GABA) Concentration of the Prefrontal Lobe in Unmedicated Patients with Obsessive-Compulsive Disorder: A Research of Magnetic Resonance Spectroscopy. *Shanghai Arch Psychiatry.* 28 (5), 263–270.

(63) Grados, M., Prazak, M., Saif, A., and Halls, A. (2016) A review of animal models of obsessive-compulsive disorder: a focus on developmental, immune, endocrine and behavioral models. *Expert Opin. Drug Discovery* 11 (1), 27–43.

(64) Oulis, P., Masdrakis, V. G., Karapoulos, E., Karakatsanis, N. A., Kouzoupis, A. V., Konstantakopoulos, G., and Soldatos, C. R. (2009) Tiagabine augmentation to fluvoxamine-risperidone combination in the treatment of obsessive-compulsive disorder. *World J. Biol. Psychiatry.* 10, 953–5.

(65) Irwin, J. J., Sterling, T., Mysinger, M. M., Bolstad, E. S., and Coleman, R. G. (2012) ZINC: a free tool to discover chemistry for biology. *J. Chem. Inf. Model.* 52, 1757–1768.

(66) GaussView, Version 4.1, Semichem, Inc., Shawnee Mission, KS, 2003.

(67) Morris, G. M., Goodsell, D. S., Halliday, R. S., Huey, R., Hart, W. E., Belew, R. K., and Olson, A. J. (1998) Automated docking using a Lamarckian genetic algorithm and an empirical binding free energy function. *J. Comput. Chem.* 19, 1639–1662.

(68) Boeckmann, B., Bairoch, A., Apweiler, R., Blatter, M.-C., Estreicher, A., Gasteiger, E., Martin, M. J., Michoud, K., O'Donovan, C., and Phan, I. (2003) The SWISS-PROT protein knowledgebase and its supplement TrEMBL in 2003. *Nucleic Acids Res.* 31, 365–370.

(69) Beuming, T., Shi, L., Javitch, J. A., and Weinstein, H. (2006) A comprehensive structure-based alignment of prokaryotic and eukaryotic neurotransmitter/Na<sup>+</sup> symporters (NSS) aids in the use of the LeuT structure to probe NSS structure and function. *Mol. Pharmacol.* *70*, 1630–1642.

(70) Skovstrup, S., Taboureau, O., Bräuner-Osborne, H., and Jørgensen, F. S. (2010) Homology modelling of the GABA transporter and analysis of tiagabine binding. *ChemMedChem* *5*, 986–1000.

(71) Morris, G. M., Huey, R., Lindstrom, W., Sanner, M. F., Belew, R. K., Goodsell, D. S., and Olson, A. J. (2009) AutoDock4 and AutoDockTools4: Automated docking with selective receptor flexibility. *J. Comput. Chem.* *30*, 2785–2791.

(72) Salat, K., and Filipek, B. (2015) Antinociceptive activity of transient receptor potential channel TRPV1, TRPA1, and TRPM8 antagonists in neurogenic and neuropathic pain models in mice. *J. Zhejiang Univ., Sci., B* *16* (3), 167–78.